

CogniSNN: A First Exploration to Random Graph Architecture based Spiking Neural Networks with Enhanced Expandability and Neuroplasticity

Yongsheng Huang¹, Peibo Duan^{1,*}, Zhipeng Liu¹, Kai Sun³, Changsheng Zhang¹, Bin Zhang¹ and Mingkun Xu^{2,*}

¹School of Software, Northeastern University, Shenyang, China

²Guangdong Institute of Intelligence Science and Technology, Zhuhai, China

³Department of Data Science & AI, Monash University, Melbourne, Australia

{2371447, 2310543}@stu.neu.edu.cn, duanpeibo@swc.neu.edu.cn, {zhangbin, zhangchangsheng}@mail.neu.edu.cn, kai.sun1@monash.edu, xumingkun@gdiist.cn

Abstract

Despite advances in spiking neural networks (SNNs) in numerous tasks, their architectures remain highly similar to traditional artificial neural networks (ANNs), restricting their ability to mimic natural connections between biological neurons. This paper develops a new modeling paradigm for SNN with random graph architecture (RGA), termed Cognition-aware SNN (CogniSNN). Furthermore, we improve the **expandability** and **neuroplasticity** of CogniSNN by introducing a modified spiking residual neural node (ResNode) to counteract network degradation in deeper graph pathways, as well as a critical path-based algorithm that enables CogniSNN to perform continual learning on new tasks leveraging the features of the data and the RGA learned in the old task. Experiments show that CogniSNN with re-designed ResNode performs outstandingly in neuromorphic datasets with fewer parameters, achieving 95.5% precision in the DVS-Gesture dataset with only 5 timesteps. The critical path-based approach decreases 3% to 5% forgetting while maintaining expected performance in learning new tasks that are similar to or distinct from the old ones. This study showcases the potential of RGA-based SNN and paves a new path for biologically inspired networks based on graph theory.

1 Introduction

Spiking neural networks (SNNs), inspired by biological nervous systems, provide enhanced biological interpretability and energy efficiency over traditional artificial neural networks (ANNs). Recently, various prominent SNN models have been developed, such as Spike VGG [Rathi and Roy, 2021], Spike ResNet [Fang *et al.*, 2021], and Spike Transformer [Zhou *et al.*, 2022]. These models maintain the performance benefits of conventional ANNs while leveraging the intrinsic energy efficiency of SNNs, achieving improved accuracy on neuromorphic datasets.

Despite substantial advancements achieved by contemporary SNNs, their fundamental architecture continues to parallel the computational graph framework of ANNs [Xie *et al.*, 2017; Xie *et al.*, 2019]. This framework diverges considerably from the brain's biological configuration, which resembles a random graph architecture (RGA). As early as the 1940s, [Turing, 1948] likened randomly connected unorganized machines to an infant's cerebral cortex, establishing the link between computational models and neuroscience. [Rosenblatt, 1958] later suggested that the setup of each organism's nervous system is primarily random and distinct at birth. The research by [Varshney *et al.*, 2011; Watts and Strogatz, 1998] showed that the nematode nervous system is a random, small-world graph with about 300 neurons, which further supports the RGA of the biological system. Besides, it is crucial to recognize that if SNN still inherits the technological framework of conventional ANN, it may encounter similar issues related to hyperparameter configuration in ANNs, such as the number of layers, leading to performance barriers. These insights urge a re-evaluation of the SNN framework through the RGA perspective.

In contrast, employing RGA in the architecture design of SNNs could be a potential solution to the aforementioned bottleneck by using graph theory to account for the spatial features of neural network topology. In practice, a similar effort was made by Xie *et al.* who performed experiments to validate that RGA-based ANNs achieved equivalent performance to computational graph-based ANN in multiple datasets [Xie *et al.*, 2019]. To our knowledge, the most related evidence comes from the investigation conducted by Yan *et al.* [Yan *et al.*, 2024] who performed a neural architecture search on SNN models, indirectly highlighting the promise of RGA-based SNNs. Despite the lack of direct studies on the feasibility of RGA-based SNNs, such intuition can be derived by comparing the phase of spike processing over all neurons in an SNN to graph signal processing, which is highly dependent on the graph structure.

Apart from simply evaluating the feasibility of RGA-based SNNs, it is eager to explore the potential of RGA-based SNNs in exhibiting **expandability** and **neuroplasticity**, which are two fundamental characteristics inherent in the architecture of the human brain, yet challenging to implement in deep learn-

ing models. Specifically, **expandability** refers to the ability to expand the graph structure to accommodate task learning. Traditional computational graph-based deep learning models also face expandability such that a model with deep layers might not perform as well as a model with shallow layers. However, this problem is even more challenging for RGA-based SNNs because of two aspects. First, a long path in the graph also leads to gradient vanishing/exploding. Although ResNet-inspired SNN approaches [Zhou *et al.*, 2024] could address this problem, they require significant real-valued computations, undermining the biologically inspired nature of SNNs. Moreover, unlike computational graphs where connections exist solely between neurons from adjacent layers, an edge in an RGA-based SNN possibly links neurons, in analogy with the computational graph, across disparate layers. The situation is even worse when the scale of the graph is large. Consequently, it results in feature dimension misalignment at a neuron, rendering pooling mechanisms ineffective.

Neuroplasticity [Demarin and Morović, 2014] refers to the capacity of an RGA-based SNN to rapidly reuse or modify the architecture to adapt to new tasks and avoid catastrophic forgetting. Drawing on strategies from ANN models, methods such as lifelong learning are viable ways to cope with this problem in computational graph-based ANNs and SNNs. More precisely, strategies to achieve this goal mainly include methods based on regularization [Li and Hoiem, 2017], replay techniques [Chaudhry *et al.*, 2021], architectural adjustments [Abati *et al.*, 2020], and knowledge distillation[Gou *et al.*, 2021]. In particular, methodologies that emphasize path adjustment, such as PathNet [Imai *et al.*, 2020], exhibit greater alignment with CogniSNN due to the absence of layer structure in RGA. However, implementing these methods in new tasks often requires searching for optimal unused paths, thus neglecting previously established paths. Moreover, the management of these paths becomes challenging due to task interference, a difficulty exacerbated when there is a significant domain shift between the source (old) tasks and the target (new) tasks.

This study introduces a cognition-aware SNN model (CogniSNN), conceived with the notion that the SNN itself possesses expandability and neuroplasticity cognition. We utilize Erdős-Rényi (ER) and Watts-Strogatz (WS) graph frameworks to structure CogniSNN, on which we develop a continual learning algorithm based on critical paths. The main contributions are as follows.

- **Expandability:** An OR Gate and a tailored pooling mechanism are proposed, where the former addresses network degradation and non-spike transmission, whereas the latter corrects feature dimension misalignment.
- **Neuroplasticity:** We develop a critical path-focused method to improve the continual learning ability of RGA-based SNNs. By utilizing betweenness centrality to identify essential pathways, CogniSNN selectively retrains the parameters associated with these pathways, mitigating catastrophic forgetting while maintaining performance on new tasks.
- Extensive experiments demonstrate that CogniSNN im-

proves accuracy by approximately 4.8%, 2.2%, and 2.6% across three datasets. Furthermore, our critical path-based continual learning algorithm allows CogniSNN to manage similar and different tasks with effective suppression of catastrophic forgetting by approximately 3.6% and 5.1%, respectively.

2 Related Work

2.1 Residual Structures in SNNs

Residual learning [He *et al.*, 2016a] is necessary for training large-scale deep neural networks. Spiking ResNet [Hu *et al.*, 2021] introduces the residual learning in SNNs for the first time, converting trained ResNet to a SNN by replacing the ReLU layers with spike neurons. On the one hand, although it is better than SNNs without residual operation, the information of residual blocks is not effectively preserved due to the activation of spike neurons after the residual operation. Therefore, when the number of layers exceeds 18, deep Spiking ResNet begins to degrade gradually. On the other hand, it does not verify whether directly trained SNN can address the degradation problem. To solve these two problems, SEW-ResNet [Fang *et al.*, 2021] places the residual operation after the spike neuron activation, and for the first time, directly trains a 152-layer SNN. However, due to the addition operation, output of the residual block is changed from spike form to integer form, which violates the principle of spike computation in SNNs, and leads to greater energy consumption. Moreover, the output is amplified infinitely as the layers deepen, leading to an extremely unstable training and computation process. MS-ResNet [Hu *et al.*, 2024] places spike neuron activation in front of the convolutional layer to minimize non-spike computation in the convolutional layer. However, the output of the residual block is still non-spiking, which leads to floating-point signal transmission in the subsequent residual branching.

2.2 Continual Learning in SNNs

Continual learning enables networks to continually learn like the human brain and adapt to dynamic environments in the real world, with the same brain-like perspective as SNNs. Recently, researchers have begun to focus on continual learning in SNNs. [Antonov *et al.*, 2022] propose a novel regularization method based on synaptic noise and Langevin dynamics, to preserve important parameters for the locally STDP-trained SNNs in continual learning. [Proietti *et al.*, 2023] achieve continual learning by using experience replay on SNNs for the first time, and perform well in class-incremental learning and task-free continual learning scenarios. Inspired by structure of the human brain and learning process in the biological systems, [Han *et al.*, 2023a] propose a self-organizing regulation network that selectively activates different sparse pathways according to different tasks to learn new knowledge. Similarly, [Shen *et al.*, 2024] utilize trace-based K-Winner-Take-All and variable threshold components to achieve selective activation of sparse neuron populations, not only in the spatial dimension but also in the temporal dimension for continual learning under specific tasks. [Han *et al.*,

al., 2023b] dynamically change the structure of SNNs to improve learning ability of the SNNs for new tasks by randomly growing new neurons and adaptively pruning redundant neurons.

Restricted by structure, some of the above approaches are not biologically plausible enough, some require extra memory usage, and some necessitate introduction of the complex selection mechanisms at the SNN layer, which greatly increases the complexity of SNN implementation. To better align with the memory processes of the human brain, we choose Learning Without Forgetting (LWF) [Li and Hoiem, 2017] as the basic method.

3 Preliminaries

3.1 Spiking Neuron

SNNs employ neurons characterized by biological dynamics to more closely emulate brain functionality. The spiking generation in such neurons is typically divided into three stages: charging, discharging, and resetting. Upon receiving an input current, a spiking neuron accumulates it as membrane potential. The charging mechanism is mathematically represented by (1).

$$H[t] = f(V[t - 1], C[t]), \quad (1)$$

where $H[t]$ is the membrane potential before discharging at moment t , $C[t]$ refers to the input current at moment t , $V[t - 1]$ is the membrane potential after discharging at moment $t - 1$, and f varies with the configuration of neurons.

At any given time t , the output of a discharging process at a neuron depends on whether the membrane potential exceeds a threshold V_{thr} . This process is expressed as (2):

$$S[t] = \Theta(H[t] - V_{thr}) = \begin{cases} 1, & H[t] \geq V_{thr} \\ 0, & H[t] < V_{thr} \end{cases}, \quad (2)$$

where $S[t]$ is the output at t , and Θ is the Heaviside step function.

Following the discharging process, the membrane potential experiences the resetting phase, which is categorized into soft and hard resetting. In this study, we employ the soft resetting approach, and this mechanism is represented by (3).

$$V[t] = H[t] - V_{thr} \cdot S[t]. \quad (3)$$

3.2 Learning Without Forgetting

LWF is a continual learning approach without using old task data, and aims to solve catastrophic forgetting of old task while learning new task.

Specifically, the method first computes the soft target Y_o using new task data X , shared parameters θ_s and old task specific parameters θ_o , where both parameters come from a well-trained model on old task. The process is shown in Eq. (4).

$$Y_o = CNN(X, \theta_s, \theta_o). \quad (4)$$

During training of the new task, the LWF method requires using $\hat{\theta}_o$ and new task specific parameters $\hat{\theta}_n$ being trained to obtain old task output Y'_o and new task output Y'_n , respectively. These two processes are shown in Eq. (5).

$$Y'_o = CNN(X, \hat{\theta}_s, \hat{\theta}_o), \quad Y'_n = CNN(X, \hat{\theta}_s, \hat{\theta}_n). \quad (5)$$

Finally, a total loss function $Loss$ is utilized to balance learning and forgetting, defined as follows:

$$Loss = \lambda L_{old}(Y_o, Y'_o) + L_{new}(Y_n, Y'_n) + R(\hat{\theta}_s, \hat{\theta}_o, \hat{\theta}_n). \quad (6)$$

The L_{new} , computed using new task output Y'_n and new task label Y_n , is used to ensure that the model learns the new task. Additionally, L_{old} , computed using the soft target Y_o and the old task output Y'_o , is used to mitigate the model's forgetting of old tasks. R is the regularization term introduced to prevent overfitting.

4 Modeling and Methodology

This study first concentrates on the implementation of the expandability of RGA-based SNNs by introducing CogniSNN, facilitated by ResNode and a tailored pooling strategy. Subsequently, we detail CogniSNN's capability to manage diverse tasks through a novel critical-path continual learning approach.

4.1 Modeling of CogniSNN

As illustrated in Fig.1, CogniSNN is designed to tackle classification tasks by integrating a triplet component to extract preliminary features from the input, a principal RGA-based module, and a full-connection classifier layer.

The triplet component comprises a convolution layer (Conv), a batch normalization layer (BN), and a spiking neuron layer (SN). In the following, we will denote this triplet by *ConvBNSN*.

The RGA-based module is modeled as a directed acyclic graph using WS or ER generators referenced in [Xie *et al.*, 2019]. With N denoted as the number of nodes, the graph is formulated as $G = \{\mathcal{V}, E\}$ where \mathcal{V} is the set of nodes with $|\mathcal{V}| = N$, and E is the set of edges. As depicted in the blue block of Fig.1, each node $v_i \in \mathcal{V}$ represents a ResNode, a variant of residual block used in [Hu *et al.*, 2021]. The design of ResNode attempts to solve the **issue** that a long propagation easily leads to the gradient vanishing or explosion. The adjacency matrix of G is A , in which $A_{i,j} = w, w \neq 0$ indicates that there exists an edge from v_i to v_j with weight w . Otherwise, $A_{i,j} = 0$. At time t , the input $I_j[t]$ to node v_j from its predecessors \mathcal{P}_j is given by the following:

$$I_j[t] = \sum_{i \in \mathcal{P}_j} \sigma(A_{i,j}) \times TP(SP(O_i[t])), \quad (7)$$

where $O_i[t]$ is the output of v_i , $\sigma(\cdot)$ is the sigmoid function, TP and SP stands for the tailored pooling and standard pooling. To avoid feature loss, SP is defined as follows:

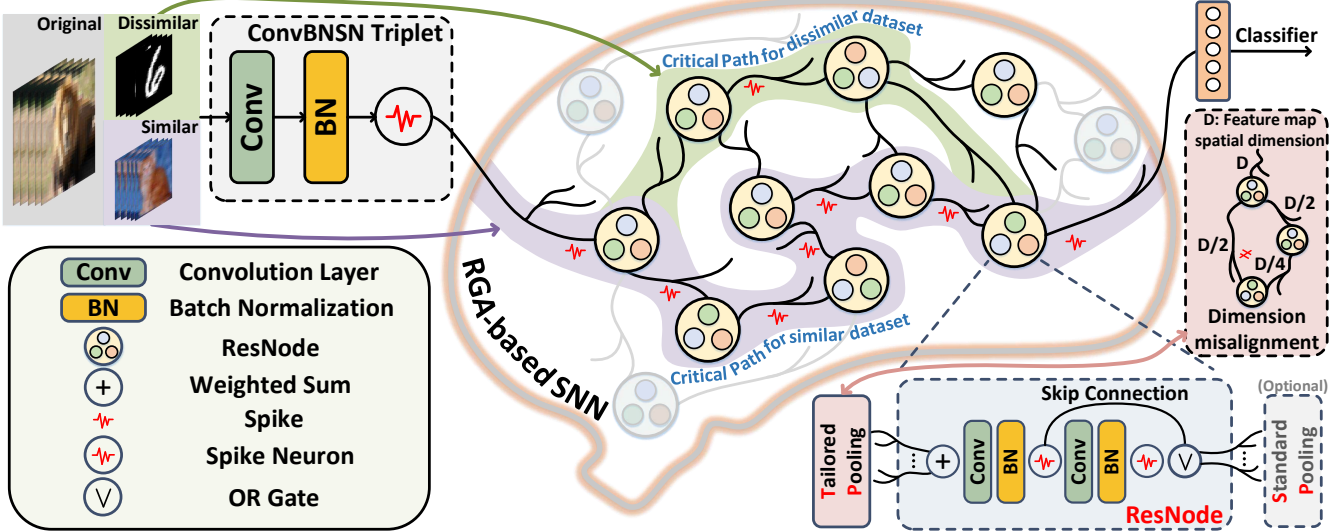


Figure 1: The overall framework of the Cognition-aware Spiking Neural Network(CogniSNN) with 7 nodes.

$$SP(O_i[t]) = \begin{cases} AvgP(O_i[t]), & D(O_i[t]) \geq \eta \\ O_i[t], & \text{Otherwise} \end{cases} \quad (8)$$

where $AvgP(\cdot)$ denotes average pooling, $D(\cdot)$ denotes the dimension of a feature map and η is a manually configured threshold set by 32 according to our experimental results. $TP(\cdot)$ aims to solve the **issue** of feature misalignment caused by random connections of the spike neuron nodes in RGA. The solutions to ResNode modeling and the tailored pooling mechanism are the keys to improving the expandability of CogniCNN. Further elaboration is provided below.

ResNode

In greater detail, v_i comprises two *ConvBNSN* triplets, which are denoted as $ConvBNSN_i^1$ and $ConvBNSN_i^2$. $ConvBNSN_i^1$ is used to transform $I_i[t]$ back into spike form. This is necessary because, as noted in (7), performing weighted operations converts $I_i[t]$ into a real-valued quantity. We then present a sophisticated skip connection that runs parallel to $ConvBNSN_i^2$ with the procedure mathematically expressed as follows.

$$\begin{aligned} O_i^1[t] &= ConvBNSN_i^1(I_i[t]) \\ O_i^2[t] &= ConvBNSN_i^2(O_i^1[t]) \\ O_i[t] &= OR(O_i^2[t], O_i^1[t]) \\ &= O_i^2[t] + O_i^1[t] - O_i^2[t] \odot O_i^1[t] \end{aligned} \quad (9)$$

In particular, $O_i^1[t]$ is derived from $ConvBNSN_i^1$ and is regarded as an identity. It is logically integrated with $O_i^2[t]$, which is obtained from $ConvBNSN_i^2$. Instead of an ADD gate, an OR gate ($OR(\cdot)$) is used because it enables the output of node $O_i[t]$ to maintain a spiking format rather than containing real values. Subsequently, $O_i[t]$ is transmitted to the

descendant nodes of v_i . Residual learning facilitates the training of deep neural networks through identity mapping [He *et al.*, 2016b]. Similarly, we have the following theorem.

Theorem 1. *The operation of an OR gate performs an identity mapping function.*

Proof. Given v_i , $O_i^2[t]$ specifies the residual mapping to be learned. By configuring the weights and biases of Batch Normalization (BN) in the second triplet to 0, or by making the attenuation constant and the activation threshold sufficiently large, we achieve $O_i^2[t] \equiv 0$. Consequently, the output from v_i becomes $O_i[t] = OR(O_i^2[t], O_i^1[t]) = OR(0, O_i^1[t]) = O_i^1[t]$, which is uniformly applied to each node. Therefore, if $O_i^1[t] = 1$, then $O_i[t] = 1$. Otherwise, $O_i[t] = 0$ under the condition $O_i^1[t] = 0$. This illustrates how the OR gate effectively achieves identity mapping. \square

Corollary 1. *OR gate operation can overcome gradient vanishing/explosion.*

Compared with ADD operation, the utilization of OR operation has the following property:

Property 1. *OR gate operation can solve the problems of non-spiking calculation and infinite amplification.*

Due to limited space, the proof of Corollary 1 and the illustration of Property 1 are given in **Section 3** of the Supplementary Material.

Tailored Pooling Mechanism

Given a node $v_j \in \mathcal{V}$ (not the root node), we estimate $D(I_j[t])$ according to the outputs from its predecessors \mathcal{P}_j as follows.

$$D(I_j[t]) = \min \{D(O_i[t]) \mid i \in \mathcal{P}_j\}. \quad (10)$$

Consequently, $TP(\cdot)$ is defined as follows:

$$TP(O_i[t]) = AvgP(O_i[t], \frac{D(O_i[t])}{D(I_j[t])}), \quad (11)$$

with the significance of implementing average pooling of $O_i[t]$ based on the kernel size $\frac{D(O_i[t])}{D(I_j[t])}$.

4.2 Critical Path-Based LWF

To capture the neuroplasticity of CogniSNN as elucidated in the Introduction, we focus on parameter fine-tuning associated with the selective substructures, termed critical paths to achieve the neural reuse to reshape functions in response to new experiences. This idea is inspired by visualizing the activation frequency of nodes. As shown in **Figure 11** of Supplementary Material, it can be observed that specific ResNodes and certain paths (defined as sequences of nodes in CogniSNN with information flow) are activated more/less frequently than others. Based on such observation, a critical path is targeted based on the concept of betweenness centrality from graph theory which is usually used to quantify the importance of a node (or edge) based on its role in connecting other nodes. In this paper, given a path p formulated as:

$$p = \{v_1, e_1, v_2, e_2, \dots, e_{l_p}, v_{l_p+1}\}, \quad (12)$$

where l_p is length of p , indicating the number of edges involved in p , we define the betweenness centrality of p , denoted by $C_B(p)$ as follows.

Definition 1. $C_B(p) = \sum_{i=1}^{l_p+1} C_B(v_i) + \sum_{j=1}^{l_p} C_B(e_j)$.

In Definition 1, $C_B(v_i)$ and $C_B(e_j)$ are the betweenness centrality of a node and an edge, which follows the principle of graph theory¹. Based on the definition of $C_B(p)$, we sort all paths in descending order according to their betweenness centrality:

$$P = \{p_1, p_2, \dots, p_{|P|}\}, \quad (13)$$

where $C_B(p_1) \geq C_B(p_2) \dots \geq C_B(p_{|P|})$, $|P|$ is the total number of paths. We then define the critical paths (\mathcal{C}) as a set of paths with capacity K according to the definition of $C_B(p)$ and the concept related to the similarity between old and new tasks, mathematically formulated as follows.

Definition 2. $\mathcal{C} \triangleq \{C_B(p_k) | k \in [1, K], K \leq |P|\}$ if two tasks are similar. Otherwise, $\mathcal{C} \triangleq \{C_B(p_k) | k \in [|P| - K + 1, |P|], K \leq |P|\}$.

To measure the similarity between the datasets, we use the Fréchet Inception Distance (FID) [Heusel *et al.*, 2017], which is originally designed to evaluate generative models by comparing the differences in the distribution of the generated and real images in the feature space. Based on empirical observations, we consider two datasets similar when their FID is below the threshold of 50. For example, CIFAR100 and CIFAR10 show strong similarity with an FID of **24.5**, while CIFAR100 and MNIST, having an FID of **2341.2**, show weak

¹The definition of node betweenness centrality and edge betweenness centrality are in **Section 4** of Supplementart Material.

Algorithm 1 The critical path-based LWF algorithm

Input: $X^+, Y^+, CogniSNN, \Theta, \Theta^+, \mathcal{I}$

Output: $CogniSNN^+$

```

1:  $CogniSNN \rightarrow CogniSNN^+$ .
2: Aligning dimensions of  $\Theta$  and  $\Theta^+$ .
3: Freeze all parameters in  $CogniSNN^+$  except for  $\theta_C$  and
    $\theta_{\Theta^+}$ .
4: for  $i \in \mathcal{I}$  do
5:   for  $\forall(x^+, y^+)$  in  $(X^+, Y^+)$  do
6:     Update  $\theta_C$  and  $\theta_{\Theta^+}$  with  $(x^+, y^+)$  using LWF.
7:   end for
8: end for
9: return  $CogniSNN^+$ 

```

similarity. This definition aligns with human cognitive processes, where principal neural pathways are leveraged for similar tasks, while unused connections are activated for unfamiliar tasks to assimilate new information and avoid forgetting prior knowledge. For simplicity, we set $K = 1$ in this study.

We design a continual learning algorithm implemented on CogniSNN by integrating critical paths and LWF method outlined in Section 3.2. The details are given in Algorithm 1. More precisely, X^+ and Y^+ are the dataset and label set in the new task. $CogniSNN$ is the model pre-trained based on the dataset in the old task. Θ and Θ^+ are classifier layers in $CogniSNN$ and $CogniSNN^+$ where $CogniSNN^+$ is the retrained $CogniSNN$ based on (X^+, Y^+) . In line 2, we align the dimensions of Θ and Θ^+ by adding or removing neurons in Θ . In line 3, we freeze all parameters except θ_C and θ_{Θ^+} that are associated with \mathcal{C} and Θ^+ . From lines 4 to 8, LWF is used to refine θ_C and θ_{Θ^+} with the dataset in the new task.

Theoretically, this critical path can be combined with many basic continual learning methods. In this paper, we only combine the more biologically plausible LWF approach for initial validation and exploration. In the future, we will combine more continual learning methods to explore the critical path more richly.

5 Experiments

5.1 Experimental Setting

We conduct experiments on three neuromorphic datasets on the NVIDIA RTX 4090 GPU. Furthermore, to demonstrate the advanced performance of CogniSNN, we engage in a detailed comparative evaluation against the SOTA SNN models, which are distinguished by architectures such as chain-like connectivity, transformer-based, and ResNet-based designs. To save space, more details of the datasets and configuration of the hyperparameters are provided in **Section 1** of Supplemental Material.

5.2 Preliminary Analysis

Before deep analysis of the performance of CogniSNN, we first assess the feasibility and potential continual learning capacity of RGA-based SNN by comparing CogniNN with a chain-structured SNN. Both are arranged with an identical

Dataset	Method	Network	Param(M)	T	Accuracy(%)
DVS-Gesture [Amir <i>et al.</i> , 2017]	SGLFormer [Zhang <i>et al.</i> , 2024]	SGLFormer-3-256	2.17	16	98.6
	Spikformer [Zhou <i>et al.</i> , 2022]	Spikformer-2-256	2.57	5	79.5
	SSNN [Ding <i>et al.</i> , 2024]	VGG-9	-	5 / 8	<u>90.7</u> / <u>94.91</u>
CIFAR10-DVS [Li <i>et al.</i> , 2017]	CogniSNN(Ours)	ER-RAG-7	0.13	5/8/16	94.8 / 95.8 / <u>98.6</u>
	CogniSNN(Ours)	WS-RAG-7	0.13	5/8/16	95.5 / 96.5 / 97.2
	Spikformer [Zhou <i>et al.</i> , 2022]	Spikformer-2-256	2.57	5	68.6
N-Caltech101 [Li <i>et al.</i> , 2017]	STSA [Wang <i>et al.</i> , 2023]	STSFormer-2-256	1.99	16	79.9
	SSNN [Ding <i>et al.</i> , 2024]	VGG-9	-	5 / 8	<u>73.6</u> / 78.6
	CogniSNN(Ours)	ER-RAG-7	1.51	5/8/16	75.8 / <u>75.9</u> / <u>76.7</u>
	CogniSNN(Ours)	WS-RAG-7	1.51	5/8/16	75.4 / <u>74.9</u> / <u>76.4</u>
	MLF[Feng <i>et al.</i> , 2022]	VGG-9	-	5	70.4
	Spikformer [Zhou <i>et al.</i> , 2022]	Spikformer	2.57	5	72.8
	SSNN [Ding <i>et al.</i> , 2024]	VGG-9	-	5/8	<u>77.9</u> / <u>79.3</u>
	CogniSNN(Ours)	ER-RAG-7	1.51	5/8	80.6 / 79.3
	CogniSNN(Ours)	WS-RAG-7	1.51	5/8	78.6 / 80.2

Table 1: Comparsion with other benchmark results on DVS-Gesture, CIFAR10-DVS, N-Caltech101.

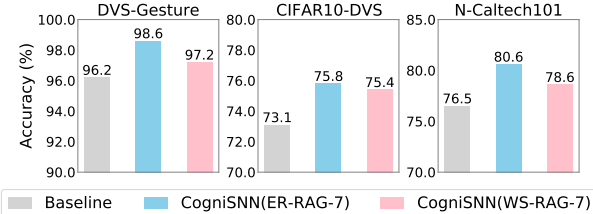


Figure 2: Comparison of results on three neuromorphic datasets between CogniSNN and chain-like structured SNN.

number of ResNodes. This preliminary analysis aims to motivate an in-depth exploration of RGA-based SNN modeling.

As for the potential of expandability, CogniSNN configured with 7 ResNodes consistently outperforms chain-structured SNNs, as seen in Figure 2. Random node connections act as implicit skip connections, dynamically prioritizing features by adjusting weights. This overcomes the limitation of sequentially increasing the dimensions of features with layers in traditional neural networks.

Model	CIFAR100	CIFAR10	CIAFR100
	source	target	benchmark
chain-like	46.3(-14.9)	31.0	61.2
CogniSNN	50.4 (-14.0)	46.1	64.4

Table 2: Neuroplasticity for RGA-based SNN in similar tasks.

Regarding neuroplasticity, we compare CogniSNN configured by 32 ResNodes with chain-like structure-based SNN under the implementation of the proposed critical path-based

Model	CIFAR100	MNIST	CIFAR100
	source	target	benchmark
chain-like	44.6(-16.6)	34.8	61.2
CogniSNN	47.5 (-16.9)	82.3	64.4

Table 3: Neuroplasticity for RGA-based SNN in dissimilar tasks.

LWF algorithm with $K = 1$. Table 2 and 3 show the performance of the critical path-based LWF applied to similar tasks ($FID = 24.5$) and dissimilar tasks ($FID = 2341.2$), respectively. In particular, CIFAR 100 is treated as source data and CIFAR10 and MNIST are treated as target data. The last column indicates the classification accuracy in the source data, serving as a benchmark for comparison. Our CogniSNN exhibits exceptional classification capabilities for new tasks, achieving a minimal accuracy decline, notably a 48% improvement in the MNIST dataset over chain-like models and a 18% increase relative to the benchmark. This illustrates the feasibility of RGA-based SNNs in the realm of continual learning.

5.3 Insightful Performance Analysis

Table 1 presents the results of the experiments conducted with CogniSNN and comparative models. Two distinct CogniSNN architectures based on ER and WS are developed, respectively. The visualization of these architectures is provided in **Section 2** of the Supplementary Material. Clearly, when tested with the time step $T = 5$, our methodology outperforms the SSNN model by 5% on DVS-Gesture, 2.2% on CIFAR10-DVS and 2.6% on N-Caltech101.

However, at $T = 8$ and $T = 16$, it should be noted that the

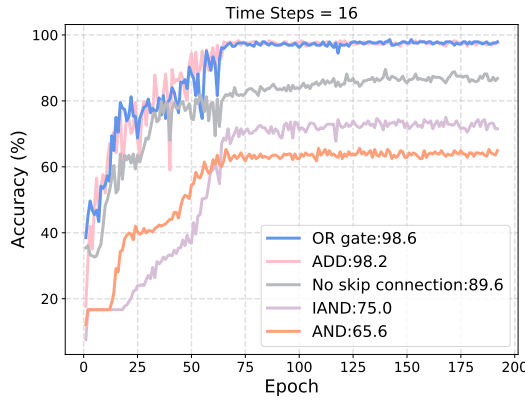


Figure 3: Comparison of results of OR and other operations on DVS-Gesture with ER-RAG-7 based CogniSNN.

performance on the CIFAR10-DVS is marginally inferior. In this regard, we believe that the graph structure is an important factor for the model performance. In future work, we will explore how to optimize the graph structure in order to achieve a better performance.

With $T = 16$, it is obvious that transformer-based SNNs (e.g., SCLFormer and STSA) demonstrate strong performance in datasets such as DVS-Gesture and CIFAR10-DVS. However, our model achieves comparable accuracy while utilizing significantly fewer parameters. For example, when evaluated on DVS-Gesture, our model requires only 1/20 of the parameters needed by the transformer-based model (0.13 million versus 2.17 million).

These improvements validate that our model not only exhibits significantly reduced latency, but also maintains accuracy even with a compact parameter scale, regardless of configuration in the time steps, demonstrating its superior adaptability and effectiveness across a diverse range of tasks.

5.4 Expandability

The expandability of CogniSNN is heavily based on the usage of skip connections within ResNodes. As described in Section 2.1, early research is generally based on the following four configurations: 1) without skip connection, 2) ADD (addition), 3) AND, and 4) IAND. We compare our skip connection (OR gate) with the four aforementioned configurations based on the ER-driven CogniSNN. Furthermore, all models with/without configuring different skip connection mechanisms are trained on the DVS-Gesture.

The experimental results are shown in Fig.3, which involve both the convergence speed and classification accuracy. It is obvious that our proposed model with an OR gate achieves a higher accuracy 9% compared to the variant without using any skip connection mechanism. This discrepancy in the accuracy measurements can be attributed to the gradient vanishing or explosion, which occurs as a result of the deep path involved in information propagation. Intriguingly, the OR gate performs similarly to the ADD operation. However, the OR gate guarantees that the outputs of ResNode are solely spike signals that will not be infinitely amplified.

5.5 Neuroplasticity

We apply the critical path-based LWF with $K = 1$ on the WS-driven CogniSNN configured with 32 ResNodes. Comparable results are observed with the ER-driven CogniSNN and are provided in **Section 6** of Supplementary Material. Tables 4 and 5 present the results, maintaining the significance of each column consistent with the corresponding column in Tables 2 and 3. The first row presents results from the application of the fine-tuned CogniSNN using traditional LWF on both tasks. The subsequent two rows display results utilizing the proposed critical path-based LWF, implemented based on paths with the highest and lowest betweenness centrality, respectively.

In Table 4, the performance of CogniSNN with fine-tuned parameters associated with the path in high C_B is marginally more effective than fine-tuned based on low C_B , showing an improvement in 0.4%. Similarly, the performance of low C_B improves 0.2% than that of high C_B in Table 5. The improvement is minor due to the simplicity of the classification task in MINST and CIFAR10. However, this supports our hypothesis regarding the correlation between the selection of the critical path and the similarity of the task (Definition 2).

Relative to the benchmark, forgetting occurs. Yet, when compared specifically to the LWF-based method, our algorithm demonstrates a 3.6% and 5.1% reduction in forgetting on the previous task. This confirms that the critical path-based LWF can effectively mitigate catastrophic forgetting.

Method	CIFAR100	CIFAR10	CIAFR100
	source	target	benchmark
LWF	44.9(-19.5)	48.0	
high C_B path	48.5(-15.9)	48.0	64.4
low C_B path	48.5(-15.9)	47.6	

Table 4: Comparison of accuracy (%) between similar tasks.

Method	CIFAR100	MNIST	CIFAR100
	source	target	benchmark
LWF	42.2(-22.2)	83.9	
high C_B path	46.6(-17.8)	85.9	64.4
low C_B path	47.3(-17.1)	86.1	

Table 5: Comparison of accuracy (%) between dissimilar tasks.

6 Conclusion

This paper validates the feasibility of RGA-based SNNs and develops a CogniSNN with expandability and neuroplasticity using the proposed ResNode, the OR gate-driven skip connection mechanism and the critical path-based LWF algorithm. The results are surprising: Compared to traditional SNNs, the CogniSNN is competitive in image recognition and continual learning. This research opens numerous exciting avenues, including leveraging the expandability of CogniSNN for continual learning by automatically adjusting its

structure, or optimizing the graph structure to enhance performance.

Ethical Statement

There are no ethical issues.

Acknowledgments

Contribution statement

References

- [Abati *et al.*, 2020] Davide Abati, Jakub Tomczak, Tijmen Blankevoort, Simone Calderara, Rita Cucchiara, and Babak Ehteshami Bejnordi. Conditional channel gated networks for task-aware continual learning. In *Proceedings of the IEEE/CVF conference on computer vision and pattern recognition*, pages 3931–3940, 2020.
- [Amir *et al.*, 2017] Arnon Amir, Brian Taba, David Berg, Timothy Melano, Jeffrey McKinstry, Carmelo Di Nolfo, Tapan Nayak, Alexander Andreopoulos, Guillaume Garreau, Marcela Mendoza, et al. A low power, fully event-based gesture recognition system. In *Proceedings of the IEEE conference on computer vision and pattern recognition*, pages 7243–7252, 2017.
- [Antonov *et al.*, 2022] DI Antonov, KV Sviatov, and Sergey Sukhov. Continuous learning of spiking networks trained with local rules. *Neural Networks*, 155:512–522, 2022.
- [Chaudhry *et al.*, 2021] Arslan Chaudhry, Albert Gordo, Puneet Dokania, Philip Torr, and David Lopez-Paz. Using hindsight to anchor past knowledge in continual learning. In *Proceedings of the AAAI conference on artificial intelligence*, volume 35, pages 6993–7001, 2021.
- [Demarin and Morović, 2014] Vida Demarin and Sandra Morović. Neuroplasticity. *Periodicum biologorum*, 116(2):209–211, 2014.
- [Ding *et al.*, 2024] Yongqi Ding, Lin Zuo, Mengmeng Jing, Pei He, and Yongjun Xiao. Shrinking your timestep: Towards low-latency neuromorphic object recognition with spiking neural networks. In *Proceedings of the AAAI Conference on Artificial Intelligence*, volume 38, pages 11811–11819, 2024.
- [ERDdS and R&wi, 1959] P ERDdS and A R&wi. On random graphs i. *Publ. math. debrecen*, 6(290-297):18, 1959.
- [Fang *et al.*, 2021] Wei Fang, Zhaofei Yu, Yanqi Chen, Tiejun Huang, Timothée Masquelier, and Yonghong Tian. Deep residual learning in spiking neural networks. *Advances in Neural Information Processing Systems*, 34:21056–21069, 2021.
- [Fang *et al.*, 2023] Wei Fang, Yanqi Chen, Jianhao Ding, Zhaofei Yu, Timothée Masquelier, Ding Chen, Liwei Huang, Huihui Zhou, Guoqi Li, and Yonghong Tian. Spikingjelly: An open-source machine learning infrastructure platform for spike-based intelligence. *Science Advances*, 9(40):eadi1480, 2023.
- [Feng *et al.*, 2022] Lang Feng, Qianhui Liu, Huajin Tang, De Ma, and Gang Pan. Multi-level firing with spiking ds-resnet: Enabling better and deeper directly-trained spiking neural networks. *arXiv preprint arXiv:2210.06386*, 2022.
- [Gou *et al.*, 2021] Jianping Gou, Baosheng Yu, Stephen J Maybank, and Dacheng Tao. Knowledge distillation: A survey. *International Journal of Computer Vision*, 129(6):1789–1819, 2021.
- [Hagberg *et al.*, 2008] Aric Hagberg, Pieter J Swart, and Daniel A Schult. Exploring network structure, dynamics, and function using networkx. Technical report, Los Alamos National Laboratory (LANL), Los Alamos, NM (United States), 2008.
- [Han *et al.*, 2023a] Bing Han, Feifei Zhao, Wenxuan Pan, Zhaoya Zhao, Xianqi Li, Qingqun Kong, and Yi Zeng. Adaptive reorganization of neural pathways for continual learning with hybrid spiking neural networks. *arXiv preprint arXiv:2309.09550*, 2023.
- [Han *et al.*, 2023b] Bing Han, Feifei Zhao, Yi Zeng, Wenxuan Pan, and Guobin Shen. Enhancing efficient continual learning with dynamic structure development of spiking neural networks. *arXiv preprint arXiv:2308.04749*, 2023.
- [He *et al.*, 2016a] Kaiming He, Xiangyu Zhang, Shaoqing Ren, and Jian Sun. Deep residual learning for image recognition. In *Proceedings of the IEEE conference on computer vision and pattern recognition*, pages 770–778, 2016.
- [He *et al.*, 2016b] Kaiming He, Xiangyu Zhang, Shaoqing Ren, and Jian Sun. Identity mappings in deep residual networks. In *Computer Vision–ECCV 2016: 14th European Conference, Amsterdam, The Netherlands, October 11–14, 2016, Proceedings, Part IV 14*, pages 630–645. Springer, 2016.
- [Heusel *et al.*, 2017] Martin Heusel, Hubert Ramsauer, Thomas Unterthiner, Bernhard Nessler, and Sepp Hochreiter. Gans trained by a two time-scale update rule converge to a local nash equilibrium. *Advances in neural information processing systems*, 30, 2017.
- [Hu *et al.*, 2021] Yangfan Hu, Huajin Tang, and Gang Pan. Spiking deep residual networks. *IEEE Transactions on Neural Networks and Learning Systems*, 34(8):5200–5205, 2021.
- [Hu *et al.*, 2024] Yifan Hu, Lei Deng, Yujie Wu, Man Yao, and Guoqi Li. Advancing spiking neural networks toward deep residual learning. *IEEE Transactions on Neural Networks and Learning Systems*, 2024.
- [Imai *et al.*, 2020] Shunsuke Imai, Shin Kawai, and Hajime Nobuhara. Stepwise pathnet: a layer-by-layer knowledge-selection-based transfer learning algorithm. *Scientific Reports*, 10(1):8132, 2020.
- [Kochen *et al.*, 1989] Manfred Kochen, Ithiel de Sola Pool, Stanley Milgram, and Theodore Mead Newcomb. The small world. (*No Title*), 1989.
- [Li and Hoiem, 2017] Zhizhong Li and Derek Hoiem. Learning without forgetting. *IEEE transactions on pattern*

- analysis and machine intelligence*, 40(12):2935–2947, 2017.
- [Li *et al.*, 2017] Hongmin Li, Hanchao Liu, Xiangyang Ji, Guoqi Li, and Luping Shi. Cifar10-dvs: an event-stream dataset for object classification. *Frontiers in neuroscience*, 11:309, 2017.
- [Loshchilov and Hutter, 2016] Ilya Loshchilov and Frank Hutter. Sgdr: Stochastic gradient descent with warm restarts. *arXiv preprint arXiv:1608.03983*, 2016.
- [Micikevicius *et al.*, 2017] Paulius Micikevicius, Sharan Narang, Jonah Alben, Gregory Diamos, Erich Elsen, David Garcia, Boris Ginsburg, Michael Houston, Oleksii Kuchaiev, Ganesh Venkatesh, et al. Mixed precision training. *arXiv preprint arXiv:1710.03740*, 2017.
- [Paszke *et al.*, 2019] Adam Paszke, Sam Gross, Francisco Massa, Adam Lerer, James Bradbury, Gregory Chanan, Trevor Killeen, Zeming Lin, Natalia Gimelshein, Luca Antiga, et al. Pytorch: An imperative style, high-performance deep learning library. *Advances in neural information processing systems*, 32, 2019.
- [Proietti *et al.*, 2023] Michela Proietti, Alessio Ragno, and Roberto Capobianco. Memory replay for continual learning with spiking neural networks. In *2023 IEEE 33rd International Workshop on Machine Learning for Signal Processing (MLSP)*, pages 1–6. IEEE, 2023.
- [Rathi and Roy, 2021] Nitin Rathi and Kaushik Roy. Diet-snn: A low-latency spiking neural network with direct input encoding and leakage and threshold optimization. *IEEE Transactions on Neural Networks and Learning Systems*, 34(6):3174–3182, 2021.
- [Rosenblatt, 1958] Frank Rosenblatt. The perceptron: a probabilistic model for information storage and organization in the brain. *Psychological review*, 65(6):386, 1958.
- [Shen *et al.*, 2024] Jiangrong Shen, Wenyao Ni, Qi Xu, and Huajin Tang. Efficient spiking neural networks with sparse selective activation for continual learning. In *Proceedings of the AAAI Conference on Artificial Intelligence*, volume 38, pages 611–619, 2024.
- [Smith, 2017] Leslie N Smith. Cyclical learning rates for training neural networks. In *2017 IEEE winter conference on applications of computer vision (WACV)*, pages 464–472. IEEE, 2017.
- [Turing, 1948] Alan Turing. Intelligent machinery (1948). *B. Jack Copeland*, page 395, 1948.
- [Varshney *et al.*, 2011] Lav R Varshney, Beth L Chen, Eric Paniagua, David H Hall, and Dmitri B Chklovskii. Structural properties of the caenorhabditis elegans neuronal network. *PLoS computational biology*, 7(2):e1001066, 2011.
- [Wang *et al.*, 2023] Yuchen Wang, Kexin Shi, Chengzhuo Lu, Yuguo Liu, Malu Zhang, and Hong Qu. Spatial-temporal self-attention for asynchronous spiking neural networks. In *IJCAI*, pages 3085–3093, 2023.
- [Watts and Strogatz, 1998] Duncan J Watts and Steven H Strogatz. Collective dynamics of ‘small-world’networks. *nature*, 393(6684):440–442, 1998.
- [West and others, 2001] Douglas Brent West et al. *Introduction to graph theory*, volume 2. Prentice hall Upper Saddle River, 2001.
- [Xie *et al.*, 2017] Saining Xie, Ross Girshick, Piotr Dollár, Zhuowen Tu, and Kaiming He. Aggregated residual transformations for deep neural networks. In *Proceedings of the IEEE conference on computer vision and pattern recognition*, pages 1492–1500, 2017.
- [Xie *et al.*, 2019] Saining Xie, Alexander Kirillov, Ross Girshick, and Kaiming He. Exploring randomly wired neural networks for image recognition. In *Proceedings of the IEEE/CVF International Conference on Computer Vision*, pages 1284–1293, 2019.
- [Yan *et al.*, 2024] Shen Yan, Qingyan Meng, Mingqing Xiao, Yisen Wang, and Zhouchen Lin. Sampling complex topology structures for spiking neural networks. *Neural Networks*, 172:106121, 2024.
- [Zhang *et al.*, 2024] Han Zhang, Chenlin Zhou, Liutao Yu, Liwei Huang, Zhengyu Ma, Xiaopeng Fan, Huihui Zhou, and Yonghong Tian. Sglformer: Spiking global-local-fusion transformer with high performance. *Frontiers in Neuroscience*, 18:1371290, 2024.
- [Zhou *et al.*, 2022] Zhaokun Zhou, Yuesheng Zhu, Chao He, Yaowei Wang, Shuicheng Yan, Yonghong Tian, and Li Yuan. Spikformer: When spiking neural network meets transformer. *arXiv preprint arXiv:2209.15425*, 2022.
- [Zhou *et al.*, 2024] Chenlin Zhou, Han Zhang, Liutao Yu, Yumin Ye, Zhaokun Zhou, Liwei Huang, Zhengyu Ma, Xiaopeng Fan, Huihui Zhou, and Yonghong Tian. Direct training high-performance deep spiking neural networks: a review of theories and methods. *Frontiers in Neuroscience*, 18:1383844, 2024.